On the Rill Net in a Slope System

AUTHOR(S):

KASHIWAYA, Kenji

On the Rill Net in a Slope System

By Kenji KASHIWAYA

(Manuscript received November 30, 1978)

Abstract

A stochastic differential equation is introduced for the theoretical analysis of rill development on a bare slope. The equation is based on two basic hypotheses; the joining probability is proportional to the number of rills and the branching probability is proportional to relative width (width/depth). It is argued in the model experiment that these hypotheses are appropriate and that the most probable number of rills is given by the steady-state solution for the equation derived from the hypotheses. It is also shown that the model is fundamentaly valid for a real bare slope in the field and that the most probable number of rills on the slope can be estimated by using the equation.

1. Introduction

The process of rill development on unvegetated slopes can be considered as the formation process of the most probable stream paths in the slope system.

It is known that the rills develop mainly by surface flows in heavy rainfalls and transform themselves by meandering, branching and joining. Some of their features have been reported by the author[1] and others.

The stream net in a drainage system similar to the rill net in a slope system has been studied by many researchers since Horton[2] (1945) and elabolate mathematical models have been also investigated (a convenient summary of them is given by Takayama[3], 1974). As for the streams on unvegetated slopes, stochastic models have been proposed for instance by Sprunt[4] (1972) and Ashida & Tanaka[5] (1976). However, most models proposed hitherto are based on the joining process and the branching process has not been taken into consideration so much. As for the models based on both processes, one for braided streams is studied by Howard et al.[6] (1970), but such models for rills on unvegetated slopes based on them have not been sufficiently studied up to date. However, the joining process and the branching process can be observed on the unvegetated slopes in the field. They can also be seen in the experiment carried out by the author[1,7]. Therefore, we have proposed a stochastic model on the development of rills based on the two processes (Kashiwaya and Okuda[8], 1977).

In this paper, we shall discuss the stochastic model, comparing it with the results of the model experiment in the laboratory and the observation and the measurement of a bare slope in the field.

2. Modeling

2.1 Stages in rill development

It is necessary to introduce a hypothetical system for systematically explaining the phenomena of rill development.

Now, idealizing the process of rill development, we shall classify the process into four stages as follows;

i) sheet flow (ensemble of countless small streaks)
ii) formation of streaks
iii) occurrence of initial rills (unit stream)
iv) formation of steady rills.

In the transition from i) to ii), streaks are shaped by secondary flow etc. on the bed in the water. From ii) to iii) the streaks develop into initial rills (unit streams) by downcutting. In the transition from iii) to iv), the rills transform themselves remarkably by meandering, joining and branching. In the course of time, they will become, what is called, steady rills.

Therefore, it is important to investigate the process from iii) to iv) for explaining the rill development.

2.2 The stochastic model for rill development

Let us investigate the idealized slope (cf. Fig. 1) for simplifying the model with some assumptions; a) the angle and the soil condition of the slope are constant, the

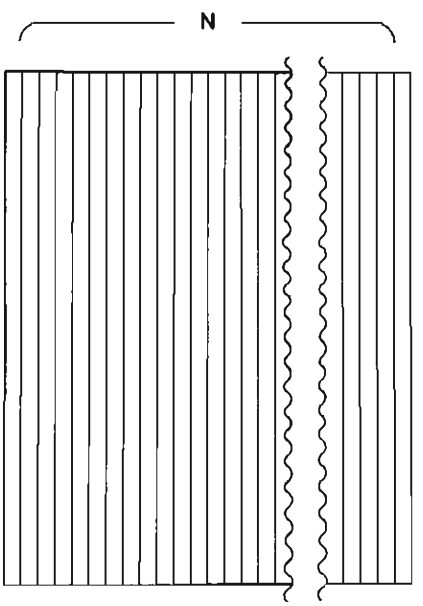

Fig. 1. A plane figure of idealized rills at the initial stage.

surface discharge per unit width is constant and the slope has a definite region, b) the number of initial rills depends on the discharge and the width and depth of all of them are equal to one another respectively, i.e. unit streams, c) the total number of unit streams is conserved and the surface flow does not permeate into the slope bed.

Taking them into consideration, we shall constitute a stochastic model based on the following two hypotheses;

A) the joining ratio of rills increases as the number of rills increases,

B) the branching ratio of rills increases as the relative width (width/depth) of rills increases.

Now, we will start with the number of initial rills N at a specified region with definite width (cf. Fig. 1 and Fig. 2). If at an instant t, the number of rills has become k in the specified portion, the probability that one rill will join with another rill in the section Δx in the interval $(t, t+\Delta t)$ is equal to

$$Q_k=\alpha(k-1)F(x)\Delta x\Delta t \tag{1-1}$$

and the probability that the rills will branch is equal to

$$R_k=\beta\sum_{i=1}^{k}\frac{w_i-w_0}{D_i}G(x)\Delta x\Delta t \tag{2-1}$$

where Q_k, R_k are the probabilities, α the joining coefficient, β the branching coefficient, w_i the width of i-th rill, w_0 the width of a unit stream, D_i the depth of i-th rill and $F(x)$, $G(x)$ the functions of slope length x (cf. Fig. 2, Fig. 3). Finally, it will be assumed that the probability that a rill will branch into more than two rills, or that more than two rills will join during $(t, t+\Delta t)$ are $O(\Delta t)$.

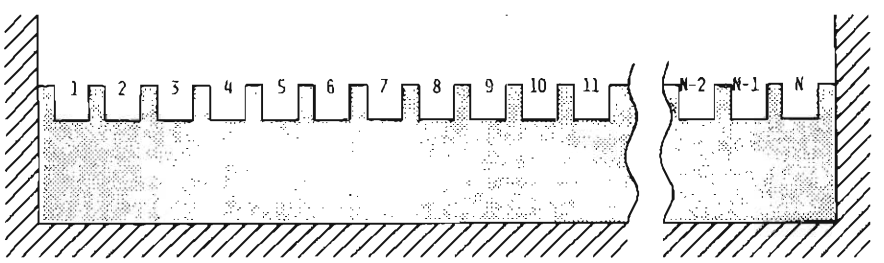

Fig. 2. A cross section of idealized rills at the initial stage.

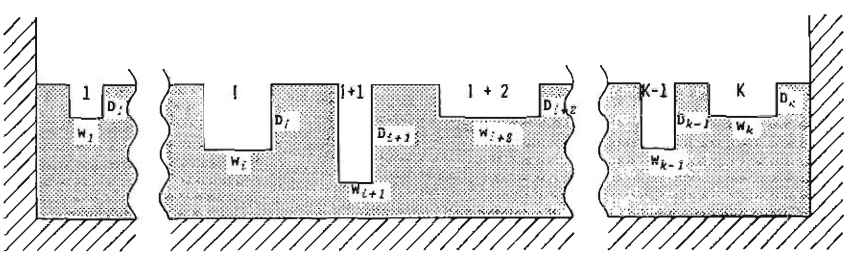

Fig. 3. A cross section of idealized rill development where k rills are represented.

We denote by $P_k(t)$ the probability that the number of rills will be k at the instant t. The probability that there are k rills in the region at time $(t, t+\Delta t)$ i.e. $P_k(t+\Delta t)$ consists of the following three probabilities;

1) $k-1$ at time t, and that a branching has occurred during $(t, t+\Delta t)$,

2) $k+1$ at time t, and that a joining has occurred during $(t, t+\Delta t)$ and

3) k at time t, and that no branching or joining has occurred during $(t, t+\Delta t)$.

Namely,

$$P_k(t+\Delta t)=R_{k-1}P_{k-1}(t)+Q_{k+1}P_{k+1}(t)+P_k(t)(1-R_k-Q_k)+O(\Delta t) \quad (3\text{–}1)$$

Considering the idealized slope shown in Fig. 1, $F(x)$, $G(x)$ and Δx can be assumed to be constant. Therefore, replacing $\alpha F(x)\Delta x$ by α', $\beta G(x)\Delta x w_0$ by β' and w_i/w_0 by w_i', eq. (3–1) become

$$P_k(t+\Delta t)=\beta'\sum_{i=1}^{k-1}\frac{w_i'-1}{D_i}P_{k-1}(t)\Delta t+\alpha' k P_{k+1}(t)\Delta t + P_k\left\{1-\alpha'(k-1)\Delta t-\beta'\sum_{i=1}^{k}\frac{w_i'-1}{D_i}\Delta t\right\} \quad (3\text{–}2)$$

Then, subtracting $P_k(t)$ from both sides, dividing them by Δt and letting $\Delta t\to 0$, we obtain the system of differential equations;

$$\frac{dP_k(t)}{dt}=\alpha' k P_{k+1}(t)+\beta'\sum_{i=1}^{k-1}\frac{w_i'-1}{D_i}P_{k-1}(t) - \left\{\alpha'(k-1)+\beta'\sum_{i=1}^{k}\frac{w_i'-1}{D_i}\right\}P_k(t) \qquad \text{for } k\neq 1,\ k\neq N \quad (4\text{–}1)$$

$$\frac{dP_1(t)}{dt}=\alpha' P_2(t)-\beta'\frac{w_1'-1}{D_1}P_1(t) \qquad \text{for } k=1 \quad (5\text{–}1)$$

$$\frac{dP_N(t)}{dt}=\beta'\sum_{i=1}^{N-1}\frac{w_i'-1}{D_i}P_{N-1}(t)-\left\{\alpha'(N-1)+\beta'\sum_{i=1}^{N}\frac{w_i'-1}{D_i}\right\}P_N(t) \qquad \text{for } k=N \quad (6\text{–}1)$$

First, we shall discuss the solution for these equations simplified as follows; the depth of rills does not change and the width of a rill is proportional to the number of unit streams involved in the rill, which means

$$D_1=D_2=\cdots\cdots=D_i=\cdots\cdots=D_N=D_0.$$

If we replace β'/D_0 by β'', eqs. (4–1), (5–1) and (6–1) will become

$$\frac{dP_k(t)}{dt}=\alpha' k P_{k+1}(t)+\beta''\sum_{i=1}^{k-1}(w'-1)P_{k-1}(t) - \{\alpha'(k-1)+\beta\sum_{i=1}^{k}(w_i'-1)\}P_k(t) \quad (4\text{–}2)$$

$$\frac{dP_1(t)}{dt}=\alpha' P_2(t)-\beta''(N-1)P_1(t) \quad (5\text{–}2)$$

$$\frac{dP_N(t)}{dt}=\beta'' P_{N-1}(t)-\alpha'(N-1)P_N(t) \tag{6-2}$$

Though these equations may be solved by using a generatinig function, we shall discuss here only the solution for steady state for them. Then, (4–2), (5–2) and (6–2) will be

$$\alpha' k P_{k+1}+\beta''\{N-(k-1)\}P_{k-1}-\{\alpha'(k-1)+\beta''(N-k)\}P_k=0 \tag{4-3}$$

$$\alpha' P_2-\beta''(N-1)P_1=0 \tag{5-3}$$

$$\beta'' P_{N-1}-\alpha'(N-1)P_N=0 \tag{6-3}$$

Let us replace β''/α' by γ and arrange these equations. Then, eq. (4–3) is transformed to

$$\gamma\{N-(k+1)\}P_{k+1}-(k+1)P_{k+2}=\gamma\{N-(k-1)\}P_{k-1}-(k-1)P_k \tag{4-4}$$

Taking eqs. (5–3) and (6–3) into consideration,

$$(k-1)P_k=\gamma\{N-(k-1)\}P_{k-1} \tag{7-1}$$

can be obtained. Hence, we obtain

$$P_2=\gamma(N-1)P_1$$

$$P_3=\frac{\gamma^2(N-1)(N-2)}{2\cdot 1}P_1$$

.....

$$P_k=\frac{\gamma^{k-1}(N-1)!}{(k-1)!(N-k)!}P_1 \tag{7-2}$$

Considering $P_1+P_2+\cdots\cdots+P_N=1$, we can obtain

$$P_1=\left(\frac{1}{1+\gamma}\right)^{N-1} \tag{8-1}$$

which yields

$$P_k=\binom{N-1}{k-1}\left(\frac{\gamma}{1+\gamma}\right)^{k-1}\left(\frac{1}{1+\gamma}\right)^{N-k} \tag{7-3}$$

This solution gives a binomial distribution.

The number of rills in the most probable state can be obtained from next condition;

$$P_{k-1}<P_k>P_{k+1} \tag{9-1}.$$

Rearranging (9–1) by substituting (7–3) into,

$$\frac{\gamma}{1+\gamma}N<k<\frac{\gamma}{1+\gamma}N+1 \tag{10-1}$$

This shows that the number of rills in the most probable state can be calculated if the value of γ and the initial number of rills N are given.

This example mentioned above shows the case where the crests on the slope are equally lowered by the collapse, etc. as the troughs are lowered. This phenomenon can be seen in the early stage of rill development or in braided streams, but it cannot be always seen at all the stages on the slope observed until now.

Then, we shall discuss the above equations by using a convenient approximation for them. As the width of a unit stream is w_0, the total width of initial rills $\sum_{i=1}^{N} w_i$ i.e. W_N is

$$\sum_{i=1}^{N} w_i = W_N = w_0 \times N \tag{11-1}$$

Setting w_i' for w_i/w_0, total width of k rills W_k becomes

$$W_k = \sum_{i=1}^{k} w_i = w_0 \sum_{i=1}^{k} w_i' \tag{12-1}$$

Replacing W_k/w_0 by W_k' and D_i/D_0 by D_i', eq. (12-1) becomes

$$W_k' = \sum_{i=1}^{k} N_i/D_i' \tag{12-2}$$

with $N_1 = w_1'D_1'$, $N_2 = w_2'D_2'$, ……, $N_k = w_k'D_k'$, where N_i is the number of unit streams in i-th rill and D_0 the depth of a unit stream and $\sum_{i=1}^{k} N_i$ is equal to N.

If we assume $D_1' = D_2' = \cdots\cdots = D_i' = \cdots\cdots = \bar{D}_k'$, eq. (2-1) can be rewritten as follows;

$$\begin{aligned} R_k &= \beta'' \sum_{i=1}^{k} \frac{w_i - 1}{\bar{D}_i'} \Delta t \\ &= \beta'' \left(\frac{W_k'^2}{W_N'} - k \frac{W_k'}{W_N'} \right) \Delta t \end{aligned} \tag{2-2}$$

Therefore, using (2-2), we can transform (4-1), (5-1) and (6-1) into

$$\begin{aligned} \frac{dP_k(t)}{dt} = {} & \alpha' k P_{k+1}(t) + \beta'' \left\{ \frac{W_{k-1}'^2}{W_N'} - (k-1) \frac{W_{k-1}'}{W_N'} \right\} P_{k-1}(t) \\ & - \left\{ \alpha(k-1) + \beta \left(\frac{W_k'^2}{W_N'} - k \frac{W_k'}{W_N'} \right) \right\} P_k(t) \end{aligned} \tag{4-5}$$

$$\frac{dP_1(t)}{dt} = \alpha' P_2(t) + \beta'' \left(\frac{W_1'}{W_N'} - \frac{W_1'}{W_N'} \right) P_1(t) \tag{5-4}$$

$$\frac{dP_N(t)}{dt} = \beta'' \left\{ \frac{W_{N-1}'^2}{W_N'} - (N-1) \frac{W_{N-1}'}{W_N'} \right\} P_{N-1}(t) - \alpha'(N-1) P_N(t) \tag{6-4}$$

For the steady state, eq. (4-5) becomes

$$k P_{k+1} - (k-1) P_k = \gamma \left\{ \left(\frac{W_k'^2}{W_N'} - k \frac{W_k'}{W_N'} \right) P_k - \left(\frac{W_{k-1}'^2}{W_N'} - (k-1) \frac{W_{k-1}'}{W_N'} \right) \right\} P_{k-1} \tag{4-6}$$

Rearranging (4–6) by substituting (5–4) and (6–4) in the steady state, we obtain

$$(k-1)P_k=\gamma\left\{\frac{W_{k-1}'^2}{W_N'}-(k-1)\frac{W_{k-1}'}{W_N'}\right\}P_{k-1} \tag{13-1}$$

Therefore, we have

$$P_k=\left(\frac{\gamma}{N}\right)^{k-1}\frac{(W_1'^2-W_1')(W_2'^2-2W_2')\cdots\cdots\{W_{k-1}'^2-(k-1)W_{k-1}'\}}{(k-1)!}P_1 \tag{13-2}$$

Then, in order to simplify these equations, we shall try to use a convenient approximation of W_k'. If the number of the rill is one, the average total width of one rill W_1' is (referring to Fig. 4)

$$W_1'=\frac{1}{N}(1+2+3+\cdots\cdots\cdots+N)=\frac{N+1}{2} \tag{14-1}$$

Assuming that each rill has the same configuration, we also have

$$W_1'=2\frac{1}{N/2}(1+2+3+\cdots\cdots\cdots+N/2)=\frac{N+2}{2}$$

$$\cdots\cdots\cdots\cdots\cdots\cdots\cdots\cdots\cdots\cdots\cdots\cdots\cdots\cdots\cdots\cdots\cdots\cdots$$

$$W_k'=k\frac{1}{N/k}(1+2+3+\cdots\cdots\cdots+N/k)=\frac{N+k}{2} \tag{14-2}$$

From these equations, we will assume an approximation of W_k' with an equation

$$W_k'=pk+q \tag{15-1}$$

where p and q are constants.

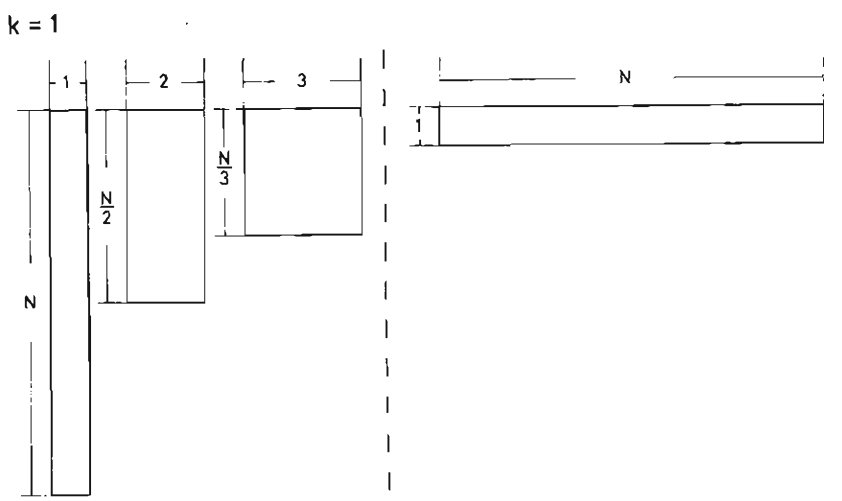

Fig. 4. Schematic representation of probable cross valley sections of the idealized rill corresponding to $k=1$, where numerals give the width of probable rills.

Substituting (15–1) into (13–2) ,one has

$$P_k=\left(\frac{r}{N}\right)^{k-1}\frac{\{(p+q)^2-(p+q)\}\{(2p+q)^2-2(2p+q)\}\cdots}{(k-1)!}$$
$$\cdots\cdots[\{p(k-1)+q\}^2-(k-1)\{p(k-1)+q\}]P_1 \qquad (13\text{–}3)$$

Then, employing the condition (9–1), the inequality $P_{k-1}<P_k$ will become

$$1<\frac{r[\{p(k-1)+q\}^2-(k-1)\{p(k-1)+q\}]}{N(k-1)}$$

Using $q=N(1-p)$ derived from (11–1) and (15–1), the above equation can be rewritten as follws;

$$\frac{2rp(1-p)-r(1-p)-1-\sqrt{\{r(1-p)+1\}^2-4rp(1-p)}}{2rp(1-p)}N+1$$
$$<k<$$
$$\frac{2rp(1-p)-r(1-p)-1+\sqrt{\{r(1-p)+1\}^2-4rp(1-p)}}{2rp(1-p)}N+1 \qquad (16\text{–}1)$$

And the inequality $P_k>P_{k+1}$ becomes

$$k<\frac{2rp(1-p)-r(1-p)-1-\sqrt{\{r(1-p)+1\}^2-4rp(1-p)}}{2rp(1-p)}N$$
$$k>\frac{2rp(1-p)-r(1-p)-1+\sqrt{\{r(1-p)+1\}^2-4rp(1-p)}}{2rp(1-p)}N \qquad (17\text{–}1)$$

Since k is positive, eqs. (16–1) and (17–1) yield

$$f(p, r, N)<k<f(p, r, N)+1 \qquad (18\text{–}1)$$

with

$$f(p, r, N)$$
$$=\frac{2rp(1-p)-r(1-p)-1+\sqrt{\{r(1-p)+1\}^2-4rp(1-p)}}{2rp(1-p)}N.$$

Thus we can estimate the number of rills for the most probable state if the values of r, p and N are given.

3. Discussion on the Theoretical Model in the Model Experiment

3.1 General remarks

Up to now, we have examined the equations which represent the development process of rills, introducing some assumptions, by regarding the process as a stochastic one.

Now, we shall test the model by experiment and discuss the calculated values

for various parameters given by the equation described above. A model experiment was employed in the test because the experimental conditions can be changed easily. It is convenient when the detailed structure of the phenomena is not known by other methods.

As the validity of the model experiment for the rill development has been reported by, for instance, Kashiwaya[7] (1976), we shall not discuss it here.

3.2 The outline of the experiment

The present experiment was carried out in a rectanguler container 120 cm long, 20 cm deep and 90 cm wide, with the water supply 20 cm from the upper end. The angle of the slope is changeable with the chain block at the upper end (cf. Fig. 5).

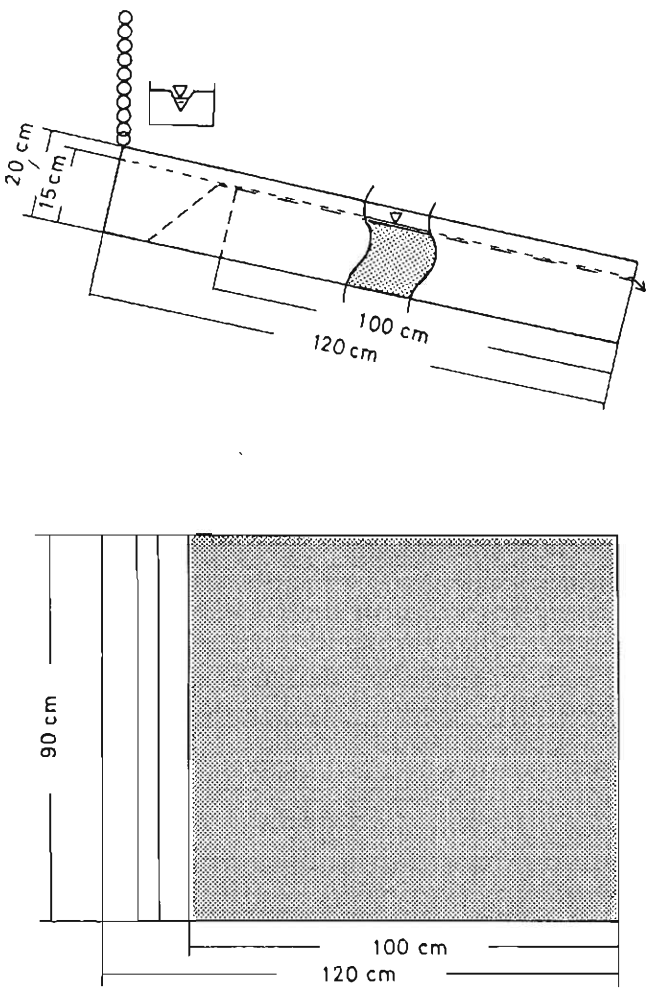

Fig. 5. Illustration of the model slope, side view and plane view.

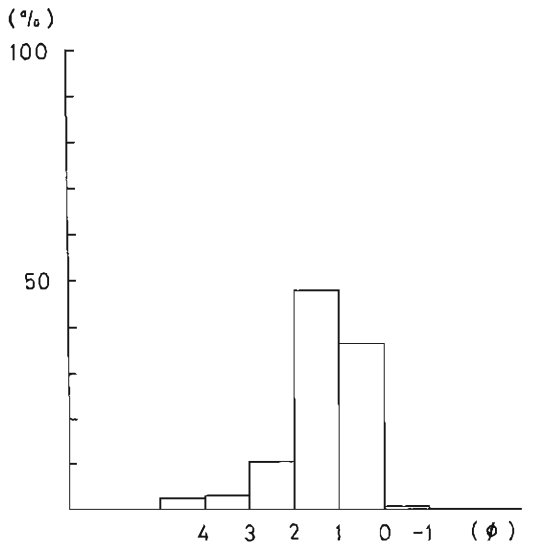

Fig. 6. Grain size distribution of soil material composing the model slope, $\phi = -\log_2 d$ with d; diameter of grain size in mm.

The container was uniformly filled with soil up to 15 cm from the bottom and the surface of the soil was made flat. The grain size of the soil used in the experiment is shown in Fig. 6, and was chosen by referring to that of the real slope. The model slope composed of the soil was mostly eroded by surface flow in the experiment and ground water runoff and interflow were rarely seen, which shows that the soil is suitable for the experiment because rill development is assumed to be caused by the surface flow.

Referring to the results of our preliminary experiment, the experiments were carried out under the conditions listed in table 1. Some stages of rill development in one case is shown in photo 1, which shows that the rills transform themselves by meandering, joining and branching and eventually become stable. A process similar to the phenomena in the photos could be observed in a series of experiments. Taking

Table 1. Experimental conditions for each respective case.

CASE	ANGLE	DISCHARGE	PERIOD
1	5°	50 cm³/sec	60 min
2	10°	50 cm³/sec	60 min
3	15°	50 cm³/sec	60 min
4	20°	50 cm³/sec	60 min
5	25°	50 cm³/sec	60 min
6	30°	50 cm³/sec	60 min

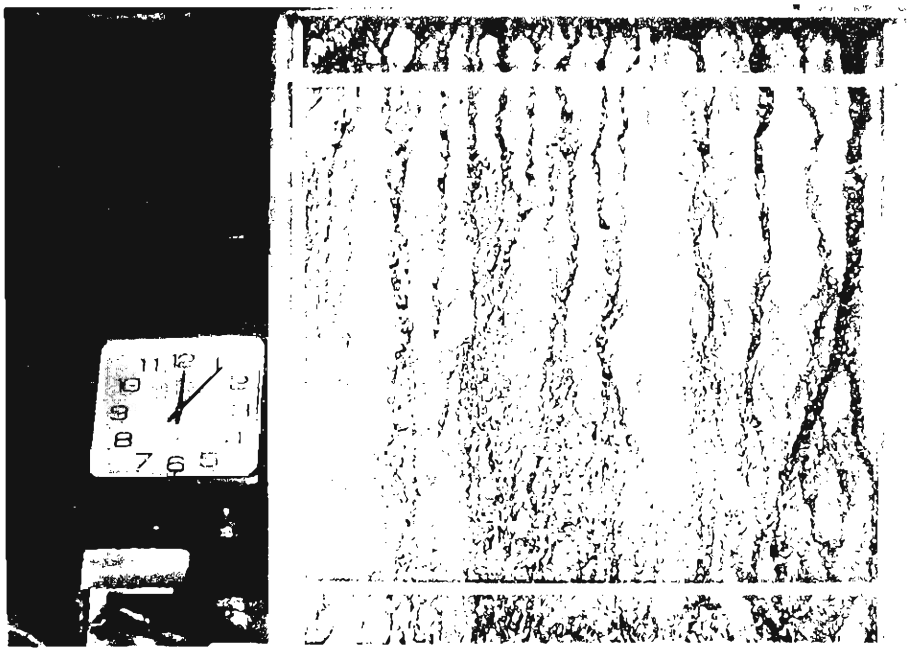

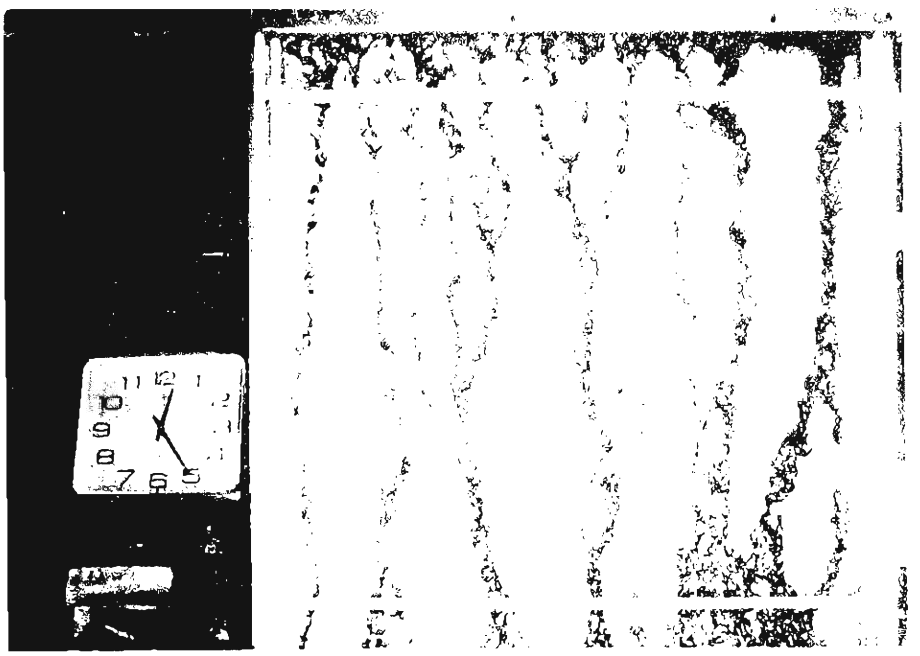

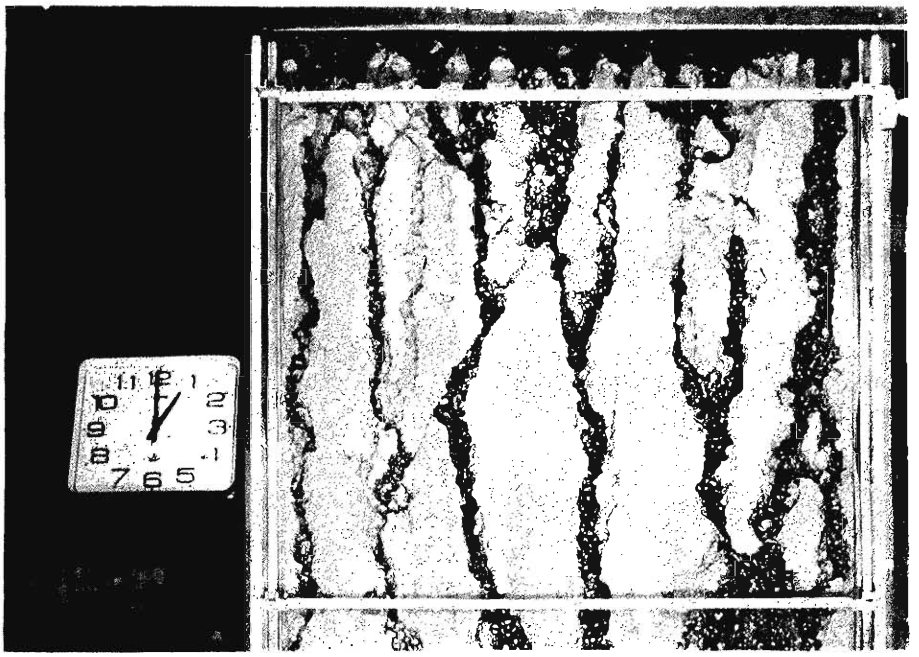

Photo 1. Development of rills in the model experiment. Appearances at 7 min, 25 min and 60 min respectively in the case of 30° after the experiment started.

the progress and the small streaks observed in the initial stage of the experiment into consideration, we can say that the idealized stages mentioned above may be appropriate.

As for measurement, the change of surface features was recorded mainly by using a 35 mm camera and 8 mm cine-camera as supplement. The relief of the slope surface was measured before starting and after finishing the experiment by using a point gauge. The supply of water was controlled with a V-notch weir. The velocity of surface flow was measured by using water-blue powder, a kind of dye, as a tracer with the 8 mm camera and a stop watch. The sediment load eroded from the surface of the bed was sampled at an appropriate time interval and weighed.

3.3 Discussion of the hypotheses on the joining probability and the branching probability

We shall discuss here the validity of eqs. (1–1) and (2–2) which involve the terms measured in the experiment. The number and the width of rills which are necessary for these equations are measured at the upper end of every 10 cm section. The number of joinings and branchings was measured in the 10 cm section. It is assumed that the joining ratio is given by the number of joinings in the section divided by the number of rills at the upper end of the same section and the branching ratio is the branchings by the number of rills in the same way (therefore, the probabilities and coefficients here are relative). This is based on the idea that the time average is

equivalent to the phase average so that the equations may match the results of the experiment. We used a time period during which the surface flows down the 10 cm section as a short interval Δt.[9]

First, the relation between the relative joining probability (joining ratio) Q_k^* and the number of rills, for instance, shown in Fig. 7 (where the slope angle is 20°) is correlative. Considering that similar results are obtained in other cases in the experiment, we may say that eq. (1–1) is acceptable. The regression line in Fig. 7 is

$$\frac{Q_k^*}{\Delta t}=0.142k+0.539 \tag{19–1}$$

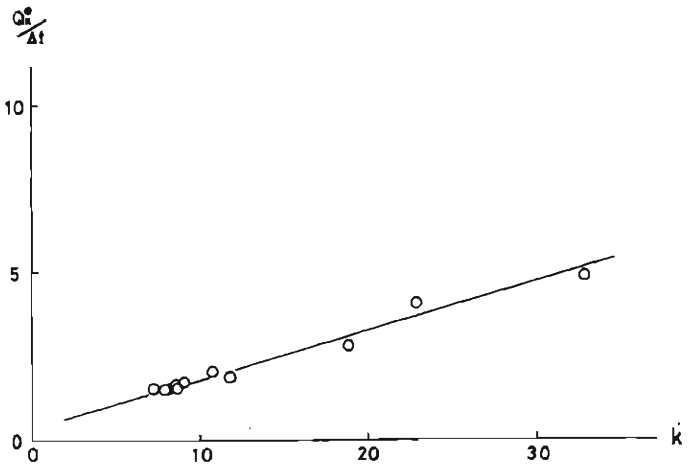

Fig. 7. Relation between the joining probability (ratio) $Q^*_k/\Delta t$ and the number of rills k.

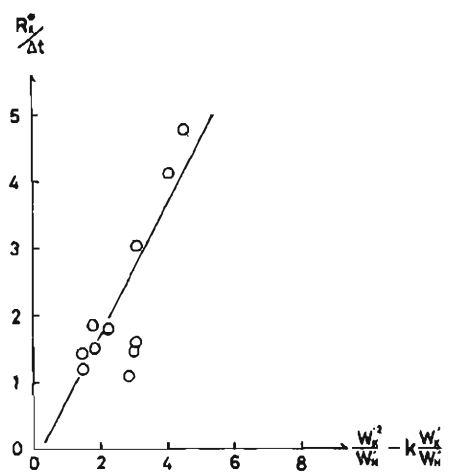

Fig. 8. Relation between the branching probability (ratio) $R^*_k/\Delta t$ and the relative width of rills $(W_k'^2/W_N')-k(W_k'/W_N')$.

The average value of Δt in this case is 0.201 sec. Therefore, the relative joining coefficient α^* is nearly 2.85×10^{-2}.

Next, let us discuss eq. (2–2). Here, we use the value of W_N' obtained in the way discussed later. The relationship between the relative width and the relative branching probability (branching ratio), for instance, shown in Fig. 8 gives a positive correlation. As similar relationships have been obtained in other cases, we recognize that eq. (2–2) is acceptable. The regression line given in Fig. 8 is

$$\frac{R_k^*}{\Delta t}=1.019\left(\frac{W_k'^2}{W_N'}-k\frac{W_k'}{W_N'}\right)-0.115 \tag{20–1}$$

where R_k^* is the relative branching probability. In this case the value of relative branching coefficient β^* is nearly 2.05×10^{-1}. Therfore, the value of $\gamma(=\beta^*/\alpha^*)$ is nearly 7.19.

As mentioned above, we can see that eqs. (1–1) and (2–2) are fairly good approximations for the phenomena. Therefore, eqs. (4–5), (5–4), (6–4) and (13–2) derived from them are proved to be applicable to the process.

3.4 Examination of the total width and the number of rills

The possibility that there is a linear relationship between the number and the total width of rills has been discussed before. An example of the experimental results examining the relationship is shown in Fig. 9 (20°). The similar results and the positive correlation obtained in other cases demonstrate that eq. (15–1) is valid as an approximate equation.

The relative total width W_N' at the initial stage is obtained by multiplying 1 by the number of initial rills which is estimated from the number of rills with which the entire surface is supposed to be covered; referring to Fig. 9, the number of k which

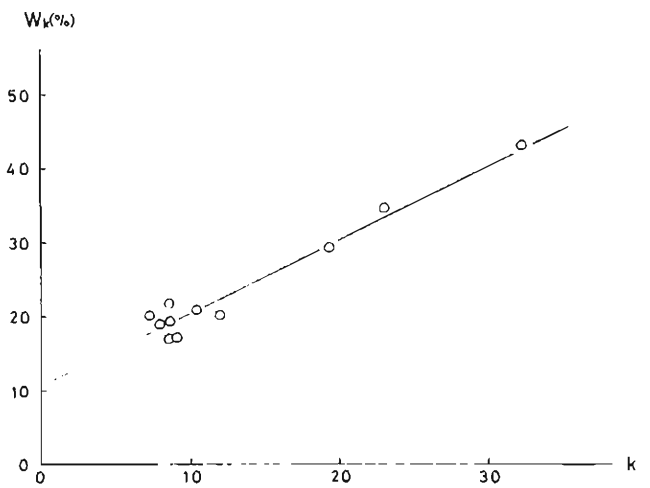

Fig. 9. Relation between the total width (per slope width) W_k and the number of rills k.

corresponds to W_N (per slope width)$=100\%$ is assumed to be the initial number of rills.

From the above results, we can see that eq. (13–3) has approximate validity.

3.5 Characters of coefficients

Next, we shall estimate γ, p and N because the most probable number of rills can be determined from the expression (18–1) by these coefficients. As for the relation between γ and the slope angle θ, it has a positive correlation as shown in Fig. 10. This means that the joining becomes more difficult as the slope angle becomes steeper and the branching becomes easier at the early stage because the depth of water becomes shallower.

Though the value of γ seems to increase rapidly from the angle 25°, a linear regression is more correlative than a quadratic regression. The regression equation represented by a straight line in Fig. 10 is

$$\gamma=0.428\theta+1.79 \tag{21–1}$$

where θ is the slope angle in degree.

The relation between p and the slope angle is shown in Fig. 11. It can be seen that the rate of increase of p decreases with the angle. In regression analysis, a quadratic regression is more correlative than a linear regression. Using the quadratic regression, the regression curve in the figure is expressed by

$$p=-1.36\times10^{-4}\theta^2+7.62\times10^{-3}\theta+8.36\times10^{-1} \tag{22–2}$$

Fig. 12 shows the relation between the number of unit streams and the slope angle. It can be seen in the figure that the number has a tendency to decrease with the angle. The number of unit streams can be thought to depend on the cross

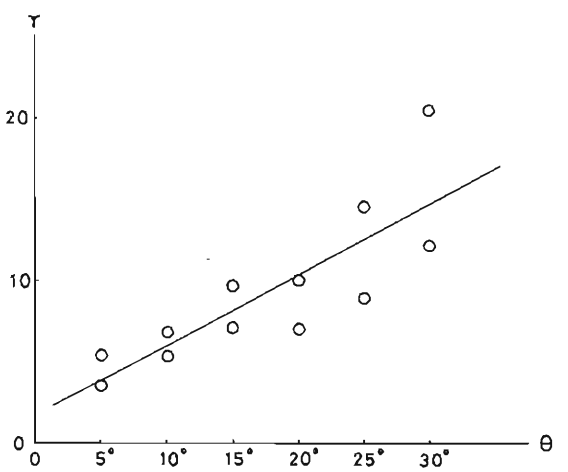

Fig. 10. Relation between γ and the slope angle (θ), where γ is the ratio of branching coefficient (β'') to joining coefficient (α').

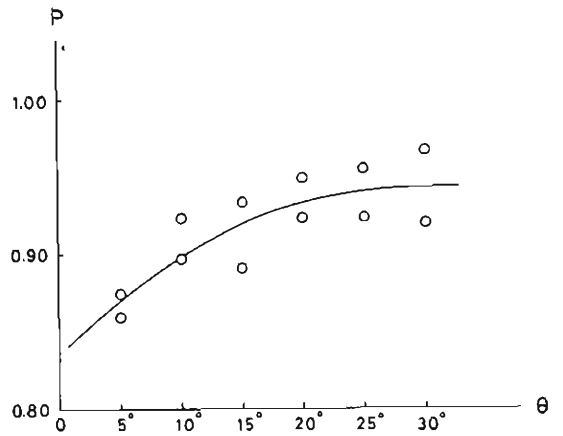

Fig. 11. Relation between the linear coefficient (p) of the width and the slope angle (θ).

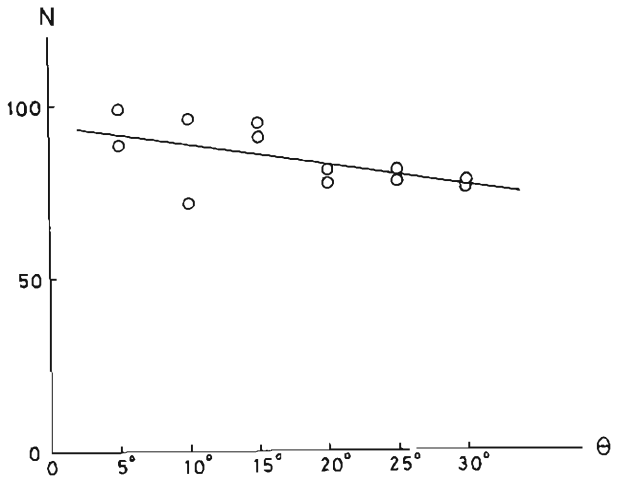

Fig. 12. Relation between the number of rills at the initial stage and the slope angle.

section of the flow as shown in Fig. 2. Therefore, as the flow velocity increases with slope angle in the experiment fixing the discharge, the cross area and the number will decrease. The regression equation in this experiment is

$$N=-0.60\theta+94.9 \tag{23-1}$$

3.6 Comparison of experimental results with calculated results

As noted above, the experimental results show that the value γ, p and N are approximately related to the slope angle θ. Thus using these relations, we can express (18–1) as a function of θ. Then, substituting $f(\theta)$ for $f(\gamma, p, N)$, the values of $f(\theta)$ can be calculated for various values of θ. As the most probable number

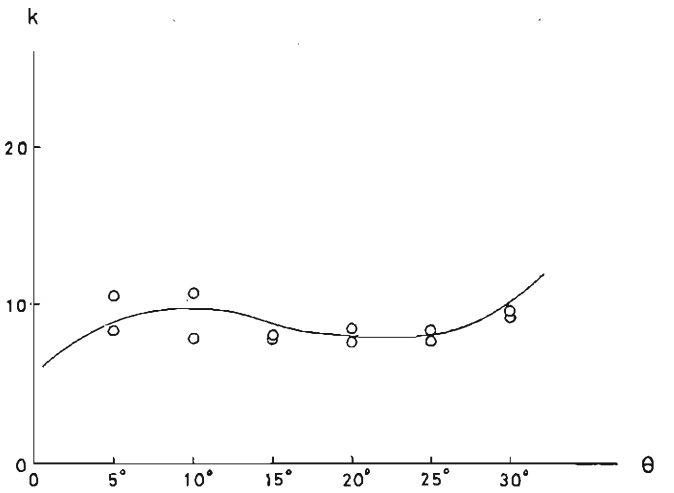

Fig. 13. Comparison of the experimental results (circles) with calculated results (curved line) in the number of rills as a function of slope angle.

of rills is given by an implicit function, $f(\theta)$ can be considered to express the most probable number.

The calculated results are shown in the curved line in Fig. 13. Experimental results are also plotted in circles in the same figure. Comparing these results, we can see that the above theory is suitable for explaining the process of rill development in the experiment.

4. Field Experiment on the Model of Rill Development

4.1 Outline of the experimental plot

The theory given above to explain the development process of rill seems to induce suitable results in the laboratory experiment. However, before accepting the theory, one must test the validity of the model in nature.

Thus, in order to test the model, an experimental plot was set on the hill slope whose surface consists of weathered granite at the side of Mt. Yokoo (Suma, Kobe city). A part of the hill slope surface was encircled into two rectangles, one 10 m wide and 20 m long (slope A) and another 2 m wide and 10 m long (slope B) (cf. photo 2). The development of rill patterning was investigated on slope A, which has a concrete partition wall except the lower end to prevent the surface flow from inflowing from outside the slope. On the other hand, hydrological factors were measured on slope B which also has a concrete partition wall with a detritus tank and a storage reservoir at the lower end (Fig. 14).

The successive change of rill topography was investigated by shooting with the 8 mm camera every 10 min. and with the 35 mm camera once and twice a week. The stereo camera P-30 was also used when the change was significant. Surface

water discharge was obtained from the measurement of water level in the storage reservoir. Sediment discharge by sheet erosion was given by weighing the load in the detritus tank with each rainfall.

4.2 Results and analysis

The surface erosion by rain water flow differs from the one by uniform sheet flow only in the point where raindrop effect must be taken into consideration. However, it is observed on this slope that rill erosion is caused mainly by the surface flow from heavy rain falls. Therefore, it is assumed that the raindrop effect can be neglected in this case. Furthermore, the runoff coefficient being constant on the whole slope, it can be so taken that the rill development at a certain place depends on the surface flow, which is proportional to the length from the upper end to the place.

From the present observation, it is recognized that the basic pattern of the rill distribution is caused by heavy rainfalls at its initial stage. In this connection, we shall discuss the rill development of Sep. 8, 1977 when the sediment load and the

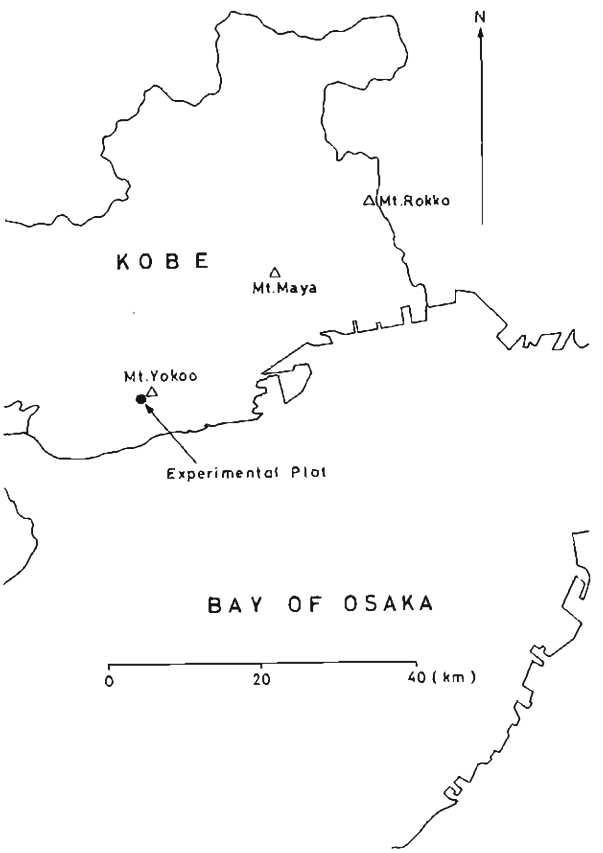

Fig. 14a. Location of the experimental plot.

surface water discharge were maximum in the present observation period. Then, the erodibility k_{ep} and the surface discharge at the lower end were obtained from the observation. On the other hand, $K_{em}v_m$ in the model slope (where the slope angle is 20°) is given in the experiment.

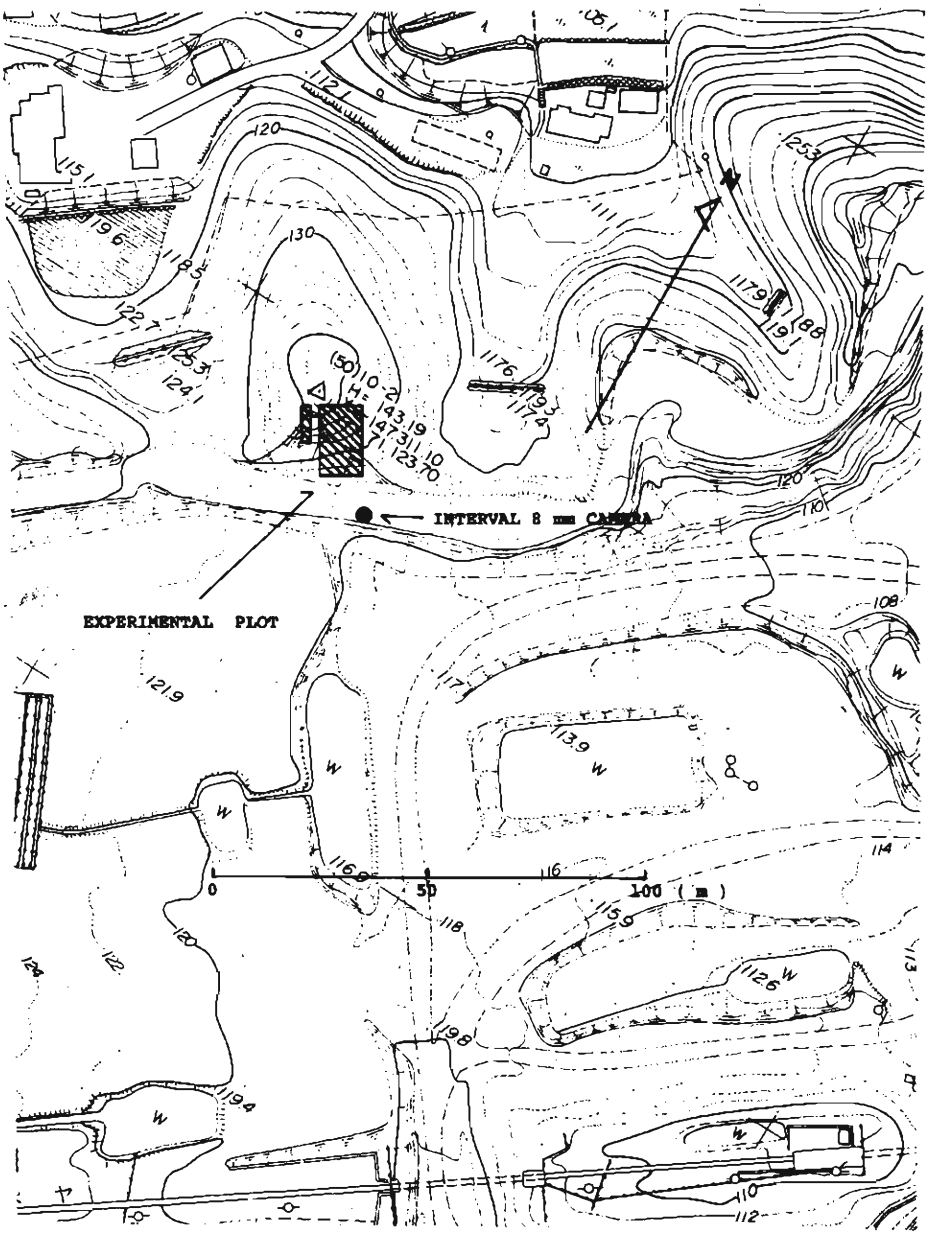

Fig. 14b. Location of the experimental plot.

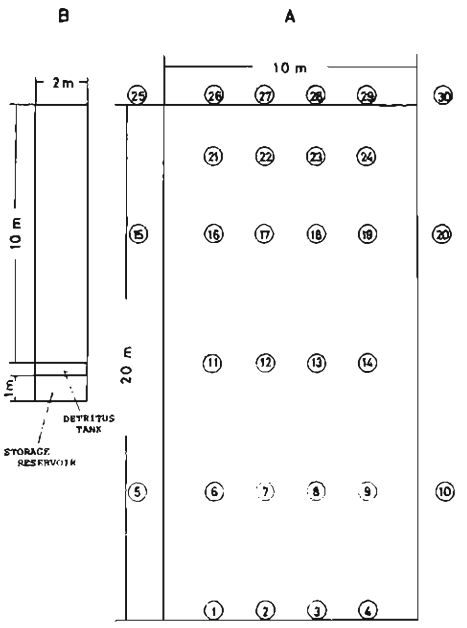

Fig. 14c. A plane figure of experimental slopes. Figures mean penetration test points.

As the dynamic similarity is expressed by

$$k_{ep}v_p=k_{em}v_m \tag{24-1}$$

where k_e is the erodibility, v the surface flow velocity and suffix p, m indicates prototype and model respectively, we can estimate the velocity when the phenomena on the real slope similar to the model happened[7]. If the surface runoff coefficient is constant on the whole slope, the distance from the upper end x where the velocity satisfies (24–1) is given by

$$v_{px}=q_x/h_x=(Ifx)/h_x \tag{25-1}$$

where q is the surface discharge per unit width, h the water depth, I the rain fall intensity, f the surface runoff coefficient and x or suffix x indicates the distance from the upper end.

From the above calculation, we obtain about 7 m for x. Therefore, we assume that the phenomena similar to the model happened at about 7 m down the slope if the other conditions are the same. Then, the relation between the number of rills and the total width per 10 m at the place is shown in Fig. 15 (circles). The solid line in the figure is derived from eq. (15–1) which shows the relation obtained in the model experiment where the slope angle is 20°.

As shown in the figure, the relation has the same tendency both in the field and in the experiment. Assuming that the relation in both places is the same, the value of p is 0.934 and N is about 83 at this place in the slope. Therefore, the value of

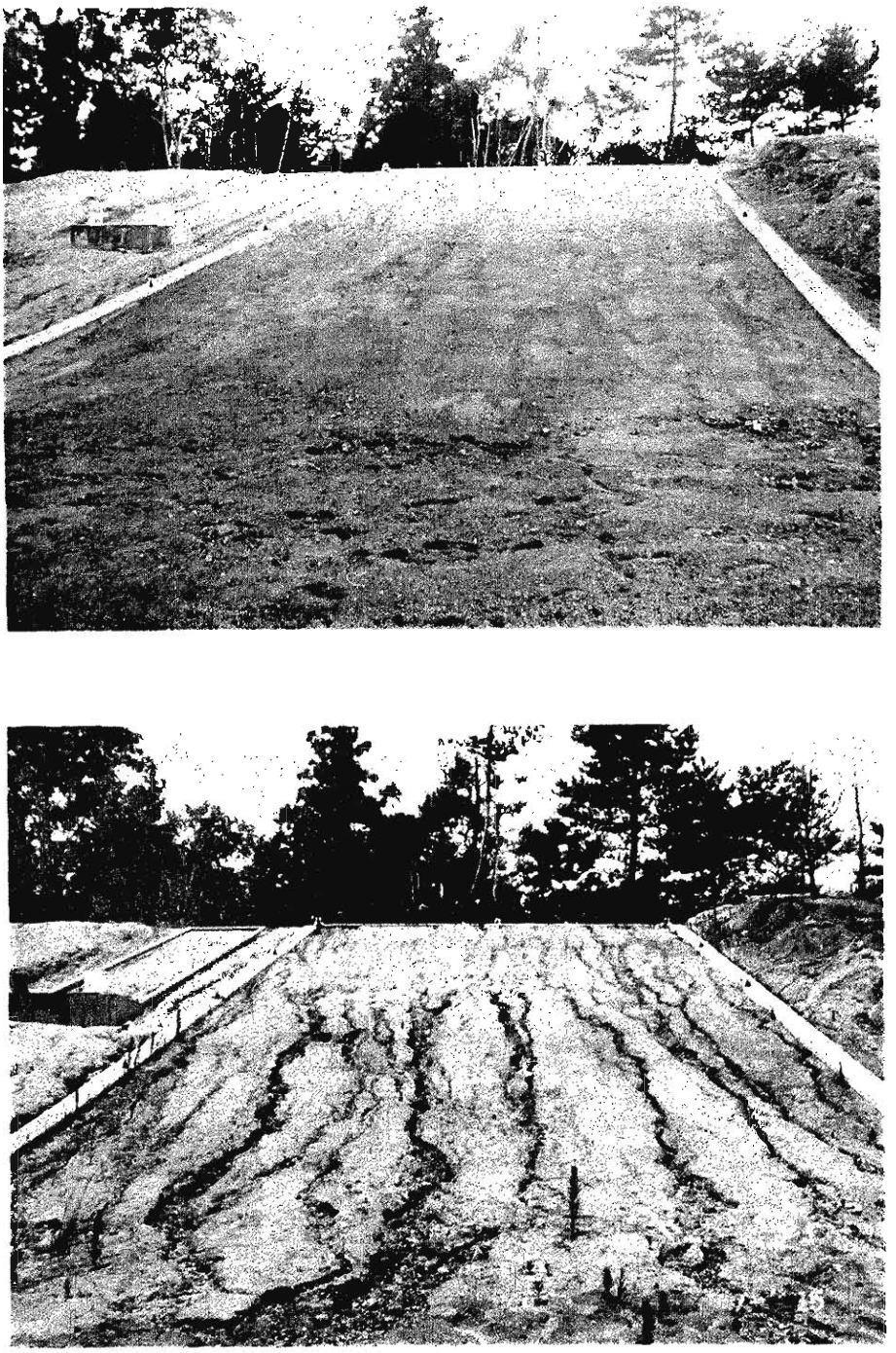

Photo 2. Experimental slopes in the field, (a) before the beginning of the observation (1977, July) and (b) at the end of the observation (1978, July).

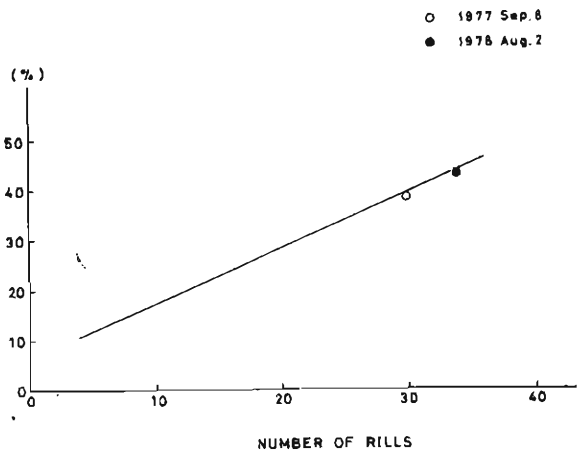

Fig. 15. Relation between total width of rills (per unit slope width) W_k and the number of rills.

N per 1 m width is about 8.3. However, the number of steady rills per 1 m width at the time when the field experiment was over (strictly speaking, the rills were not exactly steady, but the change of the pattern became very small then) was about 3.4, which was about three times as many as the calculated value of about 1. This discrepancy seems to be caused by the value of γ, and therefore the value at this place in the slope is estimated to be about three times as many as the calculated value 8–9 (cf. Fig. 10), because the number of steady rills calculated from eq. (18–1) is approximately proportional to γ at about this range.

In the model experiment mentioned above, γ seems to be roughly inverse to N (Fig. 16). Then, setting

$$\gamma = c/N \tag{26–1}$$

and substituting γ and N into the equation, we obtain about 200 for c.

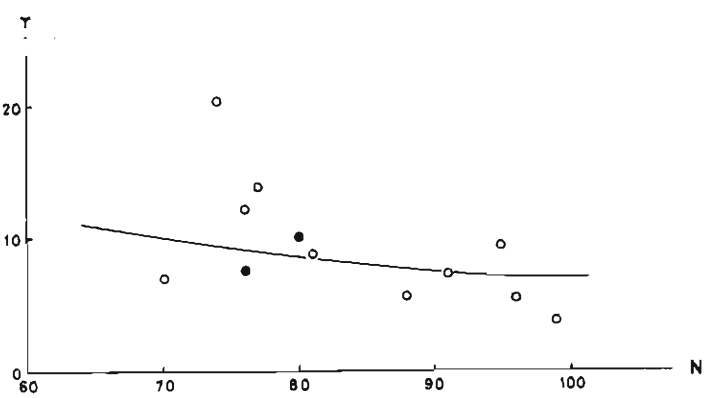

Fig. 16. Relation between γ and N (●; 20°).

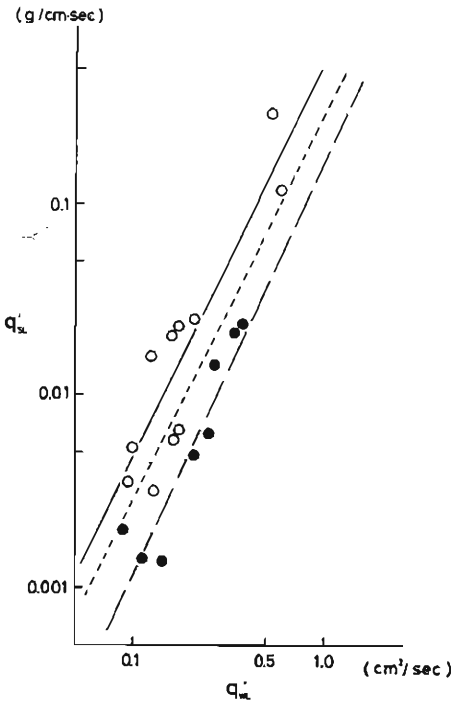

Fig. 17. Relation between sediment discharge per unit width (q_{SL}') and surface water discharge per unit width (q_{WL}'). Open circles mean the results in 1977 and black circles in 1978.

Next, we shall discuss the relation between N and slope length. Surface runoff coefficient being constant on the whole slope, the surface water discharge is proportional to the slope length. As shown in Fig. 17, sediment discharge per unit width at 10 m from the upper end of the slope is proportional to the square of the surface water discharge per unit width on this slope. Therefore, the sediment discharge per unit area may be expected to be proportional to the surface discharge, i.e., the slope length if the other conditions are the same. The initial number of rills N is subject to the size of an eroded section (cf. Fig. 3). As the eroded section corresponds to the sediment discharge per unit area, N will be proportional to the slope length. Setting 0 for N at the upper end and employing the value of N at 10 m mentioned above, we can obtain any value of N corresponding to the slope length.

4.3 Comparison of the field results with calculated results

Because the relation between γ and N, N and the slope length and the value of p are given as noted above, we can estimate the most probable number of rills at a certain position from the upper end by substituting $\gamma=200/N$ and $p=0.934$ into (18–1).

The result is shown in Fig. 18. The solid line shows the calculated result and

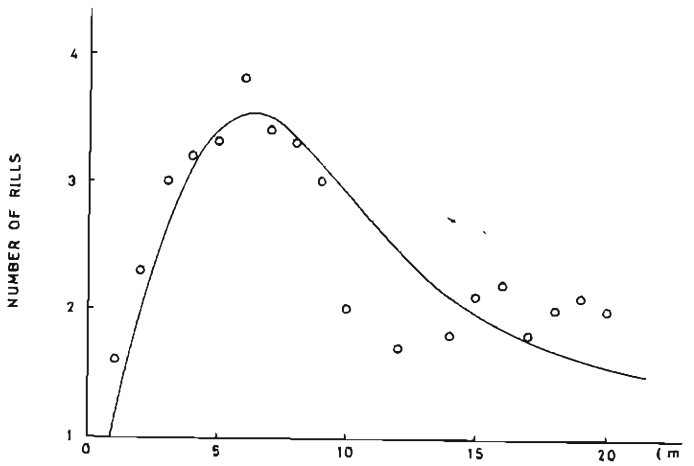

Fig. 18. Comparison of the number of rills per 1 m width measured in the field with the theoretical number of rills (the origin in the abscissa means the upper end of the slope).

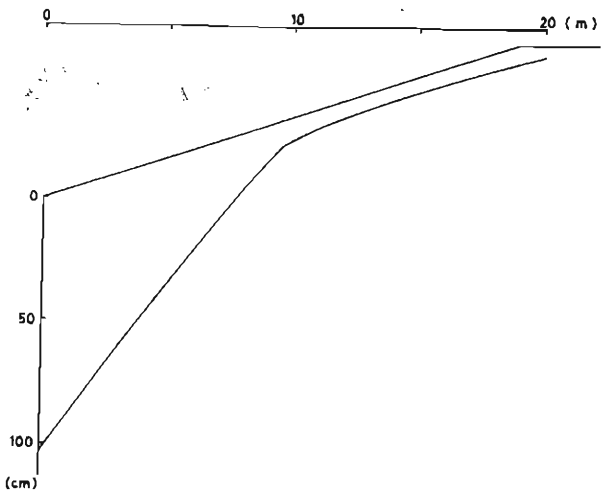

Fig. 19. The results of the cone penetration test. The curved line means the depth of the discontinuity in penetration resistance (longitudinal profile of the slope).

the circles are the observed values from the field. From this figure it is recognized that (18–1) holds to a certain degree of approximation for the field experiment. As for the deviated portion in the lower part, the result of cone penetration test (with a Doken type apparatus, a cone of diameter 3 cm driven by the impact of a 5 kg weight falling from the height of 50 cm) shows that the deviation between the observed number of rills and the theoretical one occurs in the place where the depth of the discontinuity in penetration resistance considerably changes (cf. Fig. 19). Therefore, we may well think that the deviation is caused by the local soil condition.

5. Summary and Conclusion

This paper has shown that the development of rills on a bare slope can be described by a stochastic differential equation. The rill net is different from ordinary stream nets in the point where the branching process and the joining process happen simultaneously. Therefore, both processes must be considered to derive the equation for the rill development. The equation derived theoretically was tested both in the laboratory and in the field.

The conclusion from the model experiment are as follows; in a certain region,

i) the joining ratio of rills increases with the number of rills,

ii) the branching ratio of rills increases with the relative width (width/depth) of rills,

iii) the total width of rills (per slope width) is a linear function of the number of rills and

iv) the number of steady rills obeys the steady solution for the differential equation taking i), ii) and iii) into consideration.

From the field experiment, it is shown that the steady state solution can be applied to local places on the real slope and that the number of rills in the steady state on the slope is also obtained from the solution.

Acknowledgements

The author wishes to express his hearty thanks to Professor Dr. Setsuo Okuda for helpful advice and critical reading of the manuscript. He also indebted to Dr. K. Okunishi and the members of the section of Applied Geomorphology of Disaster Prevention Research Institute of Kyoto University for helpful discussions and assistance in the experiment.

References

1) Kashiwaya, K., K. Yokoyama and S. Okuda: A Study on Gully Morphology, Geogr. Review of Japan, Vol. 47, 1974, pp. 413–425.
2) Horton, R.E.: Erosional development of streams and their drainage basins: hydrophysical approach to quantitative morphology, Geol. Soc. America Bull., Vol. 56, 1945, pp. 275–370.
3) Takayama, S.: Kasen Chikei (Fluvial Geomorphology), Kyoritsu, Co., 1974, p. 304.
4) Sprunt, B.: Digital simulation of drainage basin development, (Spatial Analysis in Geomorphology), Methun & Co., 1972, pp. 371–373.
5) Ashida, K. and K. Tanaka: A study on the stream formation process on a bare slope (1)—Around Monte Carlo simulation of stream network—, Annuals, D.P.R.I., Kyoto Univ., Vol. 18B, 1975, pp. 513–528.
6) Howard, A. D., M. E. Keetch and L. C. Vincent: Topological and geometrical properties of braided streams, W.R.R., Vol. 6, 1970, pp. 1674–1688.
7) Kashiwaya, K.: Model experiment in geomorphology—on the development of gully morphology, Geogr. Review of Japan, Vol. 49, 1976, pp. 497–504.
8) Kashiwaya, K. and S. Okuda: On stochastic model of rill pattern, Annuals, D.P.R.I., Kyoto Univ., Vol. 20 B–1, 1977, pp. 265–274.
9) Δt is not the interval given from phase velocity, but the characteristic interval in the experiment.